【固體力學（其他）】

【實驗力學】

中國機械工程學會第十三屆學術研討會・台北市・

Wavenumber Sensing Approaches by Discrete Wavenumber Transform for Active Structural Acoustic Control

Bor-Tsuen Wang

Department of Mechanical Engineering
National Pingtung Polytechnic Institute
Pingtung, Taiwan 91207

ABSTRACT

This paper presents the use of an array of accelerometers or PVDF strip sensors for wavenumber sensing approach. A simply supported beam with infinite rigid baffle subjected to a harmonic point force disturbance is considered. The PZT patches are applied as the control actuators. The discrete wavenumber transform are performed on the sensor signals so as to obtain the wavenumber transform functions (WTFs). The square modulus of any wavenumber component, corresponding to a radiation angle, in the supersonic region is defined as the cost function. The linear quadratic minimization process can then be applied to obtain the control voltage to the PZT actuator. Either the accelerometers or PVDF sensors are respectively used as error sensors to perform the wavenumber sensing approaches. Their performance in sound radiation control is studied. Results show that the wavenumber sensing approach by the DWT approach is effective. The cost function can be greatly reduced as well as the sound pressure level; therefore, the sound radiation control can be achieved. This work provides a wavenumber sensing method based on the use of piezoceramic materials and leads to enhancing the sensing ability of smart structure system for sound radiation control.

keywords: wavenumber, PVDF, accelerometer, sound radiation, sensors

I. INTRODUCTION

Wavenumber analysis has been shown an effective mean for sound radiation analysis [1]. Only the structural wavenumber components less than the acoustic wavenumber will radiate sound into the far-field, and are termed the supersonic waves. In contrast however, the subsonic waves do not contribute to sound radiation. This induces the idea of a wavenumber domain approach to the active control of structure-borne sound. Fuller and Burdisso [2] formulated a cost function, based on the wavenumber domain components associated to the angle of sound radiation to be controlled. The sound radiation can then be effectively controlled. Clark and Fuller [3] analytically demonstrated the model reference control approach in considering wavenumber transform of accelerations corresponding to the desired far-field acoustic directivity pattern. They showed that the wavenumber distributions can be largely reduced in the supersonic region; therefore, efficient sound radiation can be achieved. Maillard and Fuller [4,5] employed accelerometers as error sensors to construct the cost function, which is the wavenumber component associated with a prescribed radiation angle based on the discrete wavenumber transform.

Wang [6,7] proposed the PVDF based wavenumber domain sensing approach with the use of a series of PVDF strip sensors. The negative wavenumber components are not included for the discrete wavenumber transform (DWT) in the previous work, and thus the control effectiveness for the DWT approach is not as well as that for the continuous wavenumber transform approach. In addition, the cost function is constructed based on the summation of all supersonic wavenumber components that is related to the radiated power. This paper modifies the wavenumber domain sensing method. The implementation of the DWT approach is extended to include both the positive and negative wavenumber

components. The negative wavenumbers simply correspond to the opposite direction of sound radiation than the positive ones. Therefore, in terms of the radiation angle the structural sound radiation in both the positive and negative angles can be obtained. The cost function defined by the DWT approach can more realistically approximate that by the continuous wavenumber approach. In particular, the negative wavenumber components that corresponding to the negative radiation angle can also be selected as the cost function to be minimized. The control characteristics are, therefore, quite different from the previous work. This paper will show the formulation of the wavenumber sensing techniques for the accelerometers and PVDF strip sensors including the consideration of the negative wavenumbers. Only single wavenumber component is involved in constructing the cost function; therefore, the sound pressure level in the corresponding radiation angle to the wavenumber component can be reduced. The PVDF and accelerometers performance for different excitation frequencies are also studied and compared.

II. THEORETICAL ANALYSIS

By performing continuous wavenumber transform (CWT) in terms of spatial coordinates for a two-dimensional rectangular radiator, the acceleration wavenumber transform function $\tilde{A}$ can be obtained as follows for harmonic excitation:

$$\tilde{A}(\kappa_x,\kappa_y)=e^{j\omega t}\int_{-\infty}^{\infty}\int_{-\infty}^{\infty}\ddot{w}(x,y,t)e^{-i(\kappa_x x+\kappa_y y)}dxdy \tag{1}$$

where

$$\kappa_x=\kappa\sin\theta\cos\phi \tag{2}$$

$$\kappa_y=\kappa\sin\theta\sin\phi \tag{3}$$

and $\ddot{w}(x,y,t)$ is the acceleration of the rectangular radiator.

For a one-dimensional beam application, the y-direction response is negligible; therefore, the beam acceleration wavenumber transform function (WTF), by performing the continuous wavenumber transform and neglecting the time component, can be expressed as:

$$\tilde{A}(\kappa_x,\kappa_y)=-\omega^2\left[\frac{e^{-j\kappa_y b}-1}{-j\kappa_y}\right]\sum_{n=1}^{\infty}q_n(\omega)\tilde{\phi}_n(\kappa_x) \tag{4}$$

where

$$\begin{aligned}\tilde{\phi}_n(\kappa_x)&=\int_{-\infty}^{\infty}\phi_n(x)e^{-j\kappa_x x}dx\\&=\int_0^L\phi_n(x)e^{-j\kappa_x x}dx\\&=\alpha_n\left[\frac{1-(-1)^n e^{-i\kappa_x L}}{\alpha_n^2-\kappa_x^2}\right]\end{aligned} \tag{5}$$

in which $\phi_n(x)$ is the n-th actuator mode shape of the simply supported beam. b and L are the beam width and length respectively. The modal amplitudes $q_n(\omega)$ depend on the form of the excitation force. For a harmonic point force F applying at x_f as shown in Fig. 1, the modal amplitude can be shown as

$$q_n^f(\omega)=H_n(\omega)\phi_n^f(x_f)F \tag{6}$$

where

$$H_n(\omega)=\frac{1}{\rho_b bt_b(\omega_n^2-\omega^2)} \tag{7}$$

$$\omega_n=\alpha_n^2\sqrt{\frac{E_b I}{\rho_b bt_b}} \tag{8}$$

$$\phi_n^f(x_f)=\sin\alpha_n x_f=\sin\frac{n\pi}{L}x_f \tag{9}$$

It is noted that $\phi_n^f(x_f)$ is the displacement mode shape of the beam at coordinate x_f. For an actuator consisting of two identical piezoceramic patches, bonded symmetrically on the two opposite beam surfaces, and activated 180° out-of-phase, the corresponding modal amplitude can be derived as follows:

$$q_n^c(\omega)=H_n(\omega)\phi_n^c(x_c)M_{eq} \tag{10}$$

where

$$\phi_n^c(x_c)=\phi_n'(x_1)-\phi_n'(x_2)=2\alpha_n\sin(\alpha_n l_c/2)\phi_n(x_c) \tag{11}$$

and M_{eq} is the equivalent moment induced by the PZT actuators [8]. It is noted that $\phi_n^c(x_c)$ is the PZT actuator mode shape and represents the slope difference between the two edges of the PZT actuator at coordinates x_1, x_2. $\phi_n^c(x_c)$ can also be expressed by the displacement mode shape of the beam at the central location of the PZT patch, x_c, for the simply-supported beam. $\tilde{\phi}_n(\kappa_x)$ is the continuous wavenumber transform of $\phi_n(x)$, and can be approximated by the discrete wavenumber transform (DWT) as follows:

$$\tilde{\phi}_n(m\Delta\kappa_x)=\sum_{i=1}^{N}\phi_n(i\Delta x)e^{-j(\frac{mi}{N})}\Delta x\ , \qquad (12)$$
$$m=-(N-1),-(N-2),\ldots,-1,0,1,\ldots,N-1$$

where

$$\Delta\kappa_x=\frac{1}{L} \qquad (13)$$

$$N=\frac{L}{\Delta x} \qquad (14)$$

N is the number of discretization, i.e., the number of sensors applied in practical measurement; and Δx is the equal distance between accelerometers. The acceleration WTF by performing the DWT for $\kappa_y=0$ can then be derived:

$$\tilde{A}_{DWT}(m\Delta\kappa_x)=jb\omega^2\sum_{n=1}^{\infty}q_n(\omega)\tilde{\phi}_n(m\Delta\kappa_x), \qquad (15)$$
$$m=-(N-1),-(N-2),\ldots,-1,0,1,\ldots,N-2,N-1$$

It is noted that the negative wavenumber components (m = negative integer) are also included and simply correspond to radiation in opposite directions.

For a PVDF film arranged as shown in Fig. 1, the generated voltage can be written as [9]

$$V(x_p,t)=e^{i\omega t}K_p\sum_{n=1}^{\infty}q_n(\omega)\phi_n^p(x_p) \qquad (16)$$

where

$$\phi_n^p(x_p)=\phi_n'(x_{p1})-\phi_n'(x_{p2})=2\alpha_n\sin(\alpha_n l_p/2)\phi_n(x_p) \qquad (17)$$

in which K_p is some constant related to the material properties of the beam and PVDF film sensors [7]. It is noted that the generated voltage is proportional to the slope difference between the two edges of the PVDF film. Eq. (17) indicates that the PVDF sensor mode shape $\phi_n^p(x_p)$ is related to the displacement mode shape at the central location the PVDF sensor and weighted by the factor $2\alpha_n\sin(\alpha_n l_p/2)$.

Similarly, the generated voltages from the PVDF film shown in Eq. (16) can also be taken by the CWT in κ-plane and derived as follows:

$$\tilde{V}(\kappa_x,\kappa_y)=K_p[\frac{e^{-j\kappa_y b}-1}{-j\kappa_y}]\sum_{n=1}^{\infty}q_n(\omega)\tilde{\phi}_n^p(\kappa_x) \qquad (18)$$

where

$$\tilde{\phi}_n^p(\kappa_x)=\int_0^L\phi_n^p(x)e^{-j\kappa_x x}dx$$
$$=2\alpha_n^2\sin(\alpha_n l_p/2)[\frac{1-(-1)^n e^{-i\kappa_x L}}{\alpha_n^2-\kappa_x^2}] \qquad (19)$$

Again, the continuous wavenumber transform of the PVDF voltage shown in Eq. (18) can be approximated by the discrete wavenumber transform; therefore, the PVDF voltage WTF by performing the DWT for $\kappa_y=0$ can be obtained

$$\tilde{V}_{DWT}(m\Delta\kappa_x)=jbK_p\sum_{n=1}^{\infty}q_n(\omega)\tilde{\phi}_n^p(m\Delta\kappa_x)\ , \qquad (20)$$
$$m=-(N-1),-(N-2),\ldots,-1,0,1,\ldots,N-2,N-1$$

where

$$\tilde{\phi}_n^p(m\Delta\kappa_x)=\sum_{i=1}^{N}\phi_n^p(i\Delta x)e^{-j(\frac{mi}{N})}\Delta x\ , \qquad (21)$$
$$m=-(N-1),-(N-2),\ldots,-1,0,1,\ldots,N-2,N-1$$

$\tilde{\phi}_n^p(m\Delta\kappa_x)$ denotes the m-th wavenumber components of the PVDF mode shape $\phi_n^p(x)$ by performing the discrete wavenumber transform; and $i\Delta x$ is the spatial coordinate of the i-th sensor location.

It is noted that the mean square value of the acceleration wavenumber transform function, i.e., $|\tilde{A}|^2$, integrated over the supersonic region is related to the radiated power [1]. Only the wavenumber components satisfying $\kappa_x^2+\kappa_y^2<\kappa^2$ contribute to sound radiation into the far-field, and are termed as the supersonic waves. The other wavenumber components associated with subsonic waves do not radiate into the far-field. For a one-dimensional beam with infinite rigid baffle, the radiated power can be expressed in terms of the wavenumber transform of beam acceleration as follows [10]:

$$\Phi_p=\frac{\rho c\kappa}{4\pi\omega^2}\int_{-\kappa}^{\kappa}\frac{|\tilde{A}(\kappa_x)|^2}{\sqrt{\kappa^2-\kappa_x^2}}d\kappa_x \qquad (22)$$

It is difficult to exactly evaluate the above integral. Cremer and Heckl [10] provided an approximate method to estimate the radiated power. Here, two cost functions are defined as the square modulus of the wavenumber components corresponding to a prescribed radiation:

$$\Psi_{\kappa,\tilde{A}_{DWT}}=|\tilde{A}_{DWT}(m\Delta\kappa_x)|^2 \qquad (23)$$

$$\Psi_{\kappa,\tilde{V}_{DWT}} = |\tilde{V}_{DWT}(m\Delta\kappa_x)|^2 \quad (24)$$

It is noted that m is any positive or negative integer such that $m\Delta\kappa_x$ is in the supersonic region. The minimization of the cost function $\Psi_{\kappa,\tilde{A}_{DWT}}$ physically represents the minimization of the sound pressure level in the radiation angle corresponding to the wavenumber $m\Delta\kappa_x$. In contrast to $\Psi_{\kappa,\tilde{A}_{DWT}}$, when $\Psi_{\kappa,\tilde{A}_{DWT}}$ is chosen as the cost function that correlates to the sound pressure radiated into the far field, the sound radiation can also be controlled.

Either one of the cost functions mentioned above is obviously quadratic and positively definite and possesses a unique minimum. The linear quadratic optimal control theory (LQOCT) can then be applied to minimize the cost function, so as to find the optimal control voltages input to the piezoelectric actuators. One can easily perform minimization procedures [11] to calculate the optimal control parameters, so as to minimize the cost function. The full analysis can be referred to [12] and is omitted here for brevity.

III. RESULTS AND DISCUSSIONS

A steel beam with length of 0.38m, width of 0.04m, and thickness of 2mm is used in the simulations. The first few natural frequencies are 33.2 Hz, 128.8 Hz, 289.9 Hz, 515.4 Hz, 805.3 Hz and 1159.6 Hz. It is noted that no damping was included in the following analysis. The optimal process is suitable for controlling multiple primary sources; however, only one harmonic point force with input parameters, F=0.3N and x_f=0.067m, was considered for the following analysis. The piezoceramic patch (G-1195) [13] and PVDF films (LDT-28μk) [14] are used respectively. The piezoceramic patch is located at x_1=0.285m, x_2=0.3485m. In order to achieve the wavenumber sensing approach, a series of PVDF strip films are evenly distributed over the beam length as shown in Fig. 1. The PVDF strip film is assumed to be 0.02m in length for wavenumber sensing approaches. The number of PVDF film sensors is assumed to be 10, i.e., Δx=0.038m.

For the purpose of comparison, a series of accelerometers are also used and assumed to be located at the central location of PVDF films, so as to perform the wavenumber sensing approach. Both the radiation directivity and WTF distributions are shown to demonstrate the control mechanisms of the wavenumber sensing approaches. The radiated sound pressure is calculated at a radial distance of 3m from the beam, and plotted in dB *re* 20×10^{-6} Pa over θ=-90° to 90° for ϕ=0°. Finally, the cases of different excitation frequencies up to 1000 Hz are also simulated. The radiated powers are plotted against the excitation frequency for both before and after being controlled.

A. On-resonance excitation case, f=290Hz

Fig. 2 shows the wavenumber spectra for the use of accelerometers for excitation frequency at f=290Hz, i.e., near the third structural resonance. The thick solid denotes the disturbance response, while the thick dotted line shows the estimated disturbance response by the DWT approach. One can see that both lines agree very well; therefore, the DWT approach can properly determine the wavenumber transform function. After applying control for m=-5, m=-1, m=0, m=1, and m=5, the wavenumber spectra can be observed to be globally reduced. In particular, the wavenumber components in the supersonic region that contribute to the far field sound radiation are well attenuated. At the specified wavenumber component, the amplitude is induced to a very small value. It is noted that for the selection of positive and negative wavenumber components as the cost function the residual response are symmetry. For m=0, the reduction of the radiated power is maximum up to 62.59dB as shown in Table 1, because the wavenumber component at m=0 corresponding to the radiation angle θ=0° simply indicate the maximum sound pressure level for the third mode excitation. For m=-1 and m=1, their corresponding radiation angles are near θ=-30° and θ=30° respectively. This can be shown next in the sound pressure level distributions. For m=-5 and m=5, the specified wavenumber components are in the subsonic region. Although the wavenumber components are greatly reduced in the subsonic region, the attenuation of the wavenumber components in the supersonic region is not as much as that for other m values. Therefore, the cases of m=$\pm$5 are less efficient, only 23dB for the reduction of the radiated power. To further demonstrate the accuracy of the DWT approach, the acceleration wavenumber spectra derived from the CWT approach for the cases corresponding to the those in Fig. 2 are shown in Fig. 3. One can see both Figs. 2 and 3 agree very well. The sound pressure level distributions are shown in Fig. 4. For m=-1, 0 and 1, the sound pressure level at θ=-30°,0°, and 30° are greatly reduced respectively. For m=-5 and 5, the sound pressure level distributions are symmetry as discussed previously, and reveal higher response than other m values.

For the use of PVDF strip sensors in wavenumber sensing approaches, the cost function $\Psi_{k,\tilde{V}_{DWT}}$

is used, when m=-5, -1, 0, 1 and 5. The PVDF voltage wavenumber spectra before and after being controlled by the DWT approach are shown in Fig. 5. Again, the wavenumber components at the specified m values are greatly reduced. The corresponding acceleration wavenumber spectra are shown in Fig. 6. One can see that for m=-1, 0 and 1 the wavenumber spectra after being controlled almost identical and reveal a small dip at zero that corresponds to the radiation angle θ-0°. The wavenumber spectra are symmetry for the positive and negative m values. The sound pressure level distributions are also shown in Fig. 7. The reduction of the radiated power is also listed in Table 1. The case of m=0 can achieve the best sound radiation control for the case of third mode excitation as discussed previously.

B. Different excitation frequency performance

It is interesting to examine the performance of the accelerometers and PVDF strip sensors by wavenumber sensing approaches for different excitation frequencies. Figs. 8 and 9 show the radiated power against the excitation frequency for accelerometers and PVDF sensors respectively. Because of the symmetric response for the positive and negative m values, only the cases of m=5, m=1 and m=0 are shown. For m=0, the control can be most effective for odd mode excitation, because the specified wavenumber component corresponding to the radiation angle at θ-0° that has the maximum response for the odd mode excitation. In particular, for even mode excitation the case of m=0 will not gain any reduction of the radiated power for its physically improper detection of the sound radiation. For the cases of m=5 and m=1, a certain amount of the radiated power can also be attenuated; however, at some off-resonance excitation frequencies spillover can be observed. It is noted that the arrangement of actuators and sensors are not optimum in this work. Further investigation in optimizing the size and location of control actuator is of interest. The arrangement of the arrays of sensors, such as the number and the shape design for the PVDF sensors, need to be further studied and is out of the content of this paper.

IV. CONCLUSIONS

This paper presents an wavenumber sensing approach for structural sound radiation control in conjunction with the use of an array of accelerometers or PVDF strip sensors by the DWT approach. The wavenumber transform functions for the sensor signals are obtained by performing the DWT. The cost function can then be defined as the square modulus of a wavenumber component that corresponds to a radiation angle to the far field. Both accelerometers and PVDF sensors are shown effective for the wavenumber sensing approach by the DWT. With the proper selection of the wavenumber components in constructing the cost function, sufficient control can be achieved. However, some further work in improving the off-resonance excitation case for the wavenumber sensing approach is needed. Besides, the optimal location and sizing of PZT actuators can be of great interest and under investigation. This work provides an wavenumber domain sensing method based on the use of distributed actuators and sensors, and thus enhances the sensing ability of smart structure systems for sound radiation control.

ACKNOWLEDGEMENTS

The author gratefully acknowledges the support of the work by National Science Council, Republic of China, under grant NSC85-2212-E-020-001.

REFERENCE

1. F. Fahy, *Sound and Structural Vibration: Radiation, Transmission and Response*, (Academic Press, Inc., Orlando, Florida, 1985), pp. 72-81.
2. C. R. Fuller, and R. A. Burdisso, "A Wave Number Domain Approach to the Active Control of Structure-Borne Sound," *Journal of Sound and Vibration*, **148(2)**, 335-360 (1991).
3. R. L. Clark, and C. R. Fuller, "A Model Reference Approach for Implementing Active Structural Acoustic Control," *Journal of Acoustical Society of America*, **92(3)**, 1534-1544 (1992).
4. J. P. Maillard, and C. R. Fuller "Advanced Time Domain Wave-number Sensing for Structural Acoustic Systems. I. Theory and Design," *Journal of Acoustical Society of America*, **95(6)**, 3252-3261 (1994).
5. J. P. Maillard, J. P., and C. R. Fuller, "Advanced Time Domain Wave-number Sensing for Structural Acoustic Systems. II. Active Radiation Control of a Simply Supported Beam," *Journal of Acoustical Society of America*, **95(6)**, 3261-3272 (1994).
6. B. T. Wang, "The Evaluation of Cost Functions for Active Sound Radiation control of a Simply-Supported Beam," *Journal of the Acoustical Society of the Republic of China*, accepted for

publication (1996).
7. B. T. Wang, *The Development of PVDF Based Wavenumber Domain Model Reference Sensing Technique*, (NSC Report No. NSC84-2212-E-020-005, Taiwan, R.O.C., 1995).
8. B. T. Wang, and C. A. Rogers, "Laminate Plate Theory for Spatially Distributed INduced Strain Actuators," *Journal of Composite Materials*, **25**, 433-452 (1991).
9. J. E. Jr. Hubbard, "Distributed Sensors and Actuator for Vibration Control in Elastic Components," *Noise-Con 87*, 407-412 (1987).
10 L. Cremer, and M. Heckl, *Structure-Borne Sound: Structural Vibrations and Sound Radiation at Audio Frequencies*, (Springer-Verlag, Verlin, 1988), pp. 528-529.
11. H. C. Lester, and C. R. Fuller, "Active Control of Propeller Induced Noise Fields Inside a Flexible Cylinder," *AIAA Journal*, **28(8)**, 1374-1380 (1990).
12. B. T. Wang, *Active Structural Acoustic Control of Intelligent Material Structure System*, (NSC Report No. NSC82-0410-E-020-001, Taiwan, R.O.C., 1993), pp. 16-23.
13. Piezo Systems, Inc., *Product Catalog*, (Cambridge, Massachusetts, U.S.A., 1990)
14. Pennwalt Corporation, *Piezo Film Sensor Application Notes*, (Valley Forge, Pennsylvania, U.S.A., 1990)

Table 1. Reduction of the radiated power (dB), f=290Hz

cost function	$\Psi_{\kappa,\tilde{A}_{DWT}}$	$\Psi_{\kappa,\tilde{V}_{DWT}}$
m=-5	23.01	28.56
m=-1	28.03	51.53
m=0	62.59	58.16
m=1	28.03	51.53
m=5	23.01	28.56

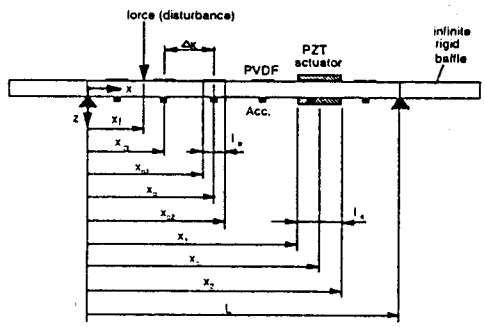

Fig. 1. The arrangement and coordinates of simply-supported beam

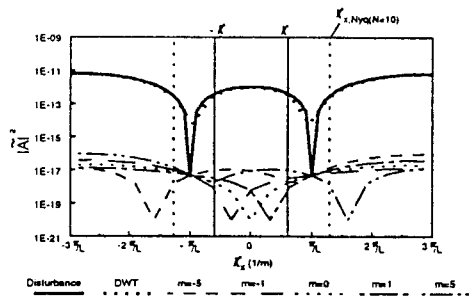

Fig. 2. Acceleration wavenumber spectra before and after being controlled for accelerometers for accelerometers for DWT approach, f=290Hz

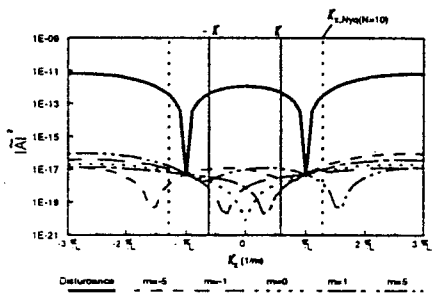

Fig. 3. Acceleration wavenumber spectra before and after being controlled for accelerometers for accelerometers for CWT approach, f=290Hz

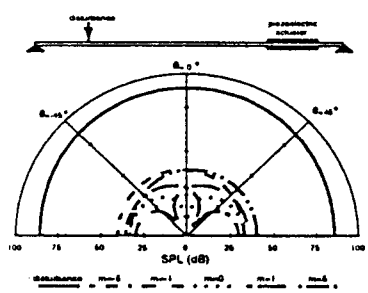

Fig. 4. Sound pressure level distribution for accelerometers, f=290Hz

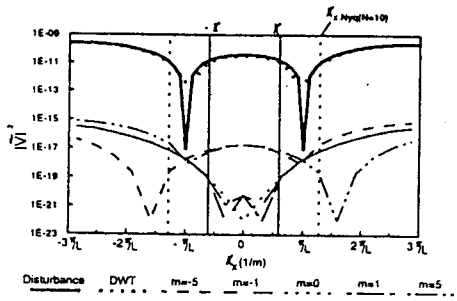

Fig. 5. PVDF voltage wavenumber spectra before and after being controlled for PVDF sensors for DWT approach, f=290Hz

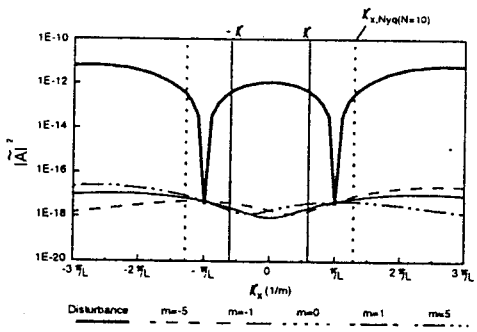

Fig. 6. Accelerometer wavenumber spectra before and after being controlled for PVDF sensors, f=290Hz

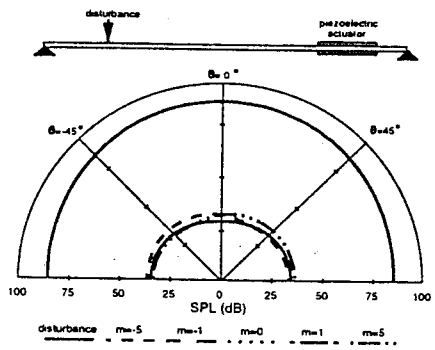

Fig. 7. Sound pressure level distribution for PVDF sensors, f=290Hz

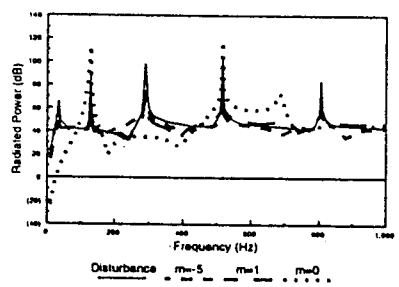

Fig. 8. Radiated power verse excitation frequency for accelerometers

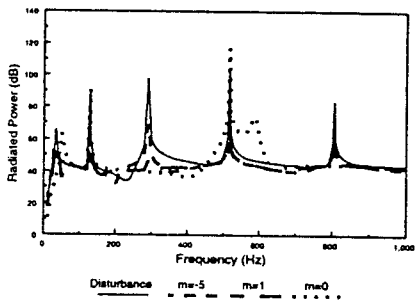

Fig. 9. Radiated power verse excitation frequency for PVDF sensors

離散波數轉換之波數感測方法於主動結構噪音控制

王栢村
國立屏東技術學院
機械工程技術系

中文摘要

本篇論文旨在以一陣列之加速度計或壓電薄膜作波數感測，考慮一具無限長剛體屏障之簡支樑，受簡諧外力激振，以壓電片為驅動器，將感測器信號取離散波數轉換以求取波數轉換函數，並以在超音波域之任一個波數平方值定義為成本函數，再以最小平方求小值法可求得輸入壓電驅動器之控制電壓，分別以加速度計及壓電薄膜進行波數感測，並評估二者在聲音幅射控制之效果。結果顯示對應於波數方位角之聲壓及成本函數均可大幅降低，因此以離散波數轉換之波數感測可達到控制效果。本文提供以壓電材料為基礎之波數感測方式，加強了智慧型材料結構系統在主動噪音控制之感測能力。

關鍵詞：波數、壓電薄膜、加速度計、聲音幅射、感測器